Zinreich SJ, Wang H, Epstein JI, Kim WS, Brem H, Anderson,JH, Ahn HS, and Rosenbaum AE. "Carotid bifurcation imaging model for more accurately comparing imaging techniques." Acta Radiologica, 369:24-28, 1986.

ACTA RADIOLOGICA

SUPPLEMENTUM 369

XIII SYMPOSIUM NEURORADIOLOGICUM STOCKHOLM JUNE 23–28, 1986

Edited by

TORGNY GREITZ

Sten Cronqvist, Kaj Ericson, Tomas Hindmarsh and Melker Lindqvist

STOCKHOLM 1986

FROM THE NEURORADIOLOGY DIVISION OF THE RUSSELL H. MORGAN DEPARTMENT OF RADIOLOGY AND RADIOLOGICAL SCIENCE, AND THE DEPARTMENTS OF PATHOLOGY AND NEUROSURGERY, THE JOHNS HOPKINS MEDICAL INSTITUTIONS, BALTIMORE, MARYLAND, USA.

CAROTID BIFURCATION IMAGING MODEL FOR MORE ACCURATELY COMPARING IMAGING TECHNIQUES

S. J. ZINREICH, H. WANG, J. I. EPSTEIN, W. S. KIM, H. BREM, J. H. ANDERSON, H. S. AHN and A. E. ROSENBAUM

Abstract

For comparing current and presubably forthcoming imaging modalities, a carotid bifurcation model was made from cadaveric specimens. Perfusing and pulsing the immersed common carotid artery and its proximal branches via a Harvard pump simulated clinical imaging conditions. Film-screen (F-S) and digital subtraction (DS) angiography, computed tomography (CT), ultrasound and magnetic resonance imaging (MRI) were compared. For CT and MRI, scanning parameters such as slice thickness, degree of overlapping, amount of contrast medium needed, scanning mode and multiplanar and three-dimensional techniques enabled enhancing the capacity for CT in the clinical setting. Direct axial CT proved to be most accurate for assessing the contours and magnitude of carotid narrowing. Nonetheless, these serial segments were not readily compared with F-S and DS angiographic full length images. The use of multiplanar reconstruction (MPR) and three-dimensional (3-D) CT achieved this and furthermore showed the external contour of the diseased segment. Concerning carotid ulceration, our carotid model study showed CT to be equally accurate with DS and superior to F-S angiography. However, in our clinical study of 34 carotid arteries in 17 patients ulcerations were equally well identified by CT and angiography but DS angiography proved superior in identifying ulcers not seen with CT. Perhaps this discrepancy is explained by the clinical routine of attaining multiple fluoroscopically positioned views of the common carotid bifurcations in DS catheter angiography unlike the complexity of attaining optimal views of tortuous vessels on CT.

The angiographic evaluation of the carotid arterial system via computed tomography (CT) has usually been displayed in the axial plane. These axial sections have even proved capable of detecting intimal disease of the carotid bifurcation not seen on angiography (6). Previously, the axial CT images have displayed the carotid vessels segmentally rather than as a full length structure as visualized by conventional angiography. Magnetic resonance imaging (MRI) in multiple planes might further facilitate this demonstration.

For more objectively comparing the various imaging modalities, a model was developed using cadaveric carotid bifurcations coupled by tubing to a Harvard pump which provided a pulsatile system during imaging.

Comparative imaging of the carotid model was then planned for: Computed tomography (CT) using primary axial, secondary multiplanar reconstruction (MPR) and three-dimensional (3-D) techniques, magnetic resonance imaging (MRI), digital subtraction (DS) and film-screen (F-S) angiography and ultrasonograpy. After these imaging studies were completed, the cadaveric carotid artery lumen was exposed and examined independently by neurosurgeon, pathologist, and neuroradiologist. This communication relates these investigations and their clinical utility.

Material and Methods

Equipment

Imaging was obtained with the following instrumentation:

Angiography was performed on a Philips Biplane Poly-I with a Puck UD changer using Medichrome film and a 0.2 mm focal spot for direct magnification. Digital subtraction angiography was done with a Philips DVI-2 with a 512×512 matrix and 0.6 mm focal spot.

Computed tomography. A Somatom DR3 was used with a 512×512 matrix and version E software for direct axial images and multiplanar reconstructions. CT scanning was performed using the following parameters: 4 mm slice thickness, 3 mm table incrementation, 0° gantry angulation, 450 mAs, 125 kVp, 256×256 matrix image data acquisition and 512×512 matrix image display. Several scanning parameters were explored to determine the most satisfactory and practical regional coverge for accomplishing rapidity of examination and multiplanar reconstructions. For the 3-D reconstructions a dedicated system, the Cemax 1000, was used. It afforded both transparency and rotational display programs.

Magnetic resonance imaging was performed with a Technicare 0.6 T scanner using the 256×256 matrix and a saddle-shaped surface coil.

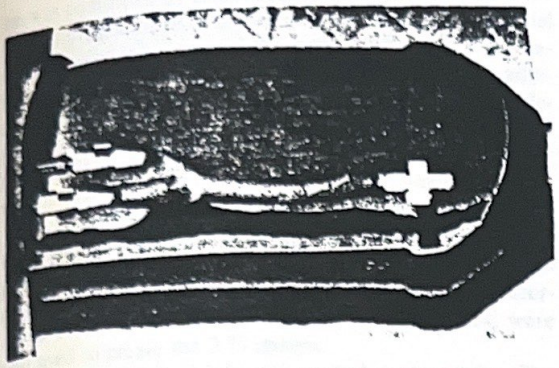

Fig. 1. Carotid model. Within a plastic bottle from which one side was removed, a cadaveric common carotid bifurcation was centered within it. The ends of the carotid segments were fitted with connectors, sutured and joined to plastic tubing and a Harvard pump. The container was then filled with saline.

Fig. 2. Cemax 3-D of both common carotid bifurcations. With the cervical spine in the background, separately colored carotid arteries were depicted. There is a pseudoaneurysm of the internal carotid artery on the left and the right carotid artery is normal.

Fig. 3. Cemax 'transparent 3-D' of the cervical carotid arteries. Transparency of the mandible where the carotid branches lie beneath it affords improved demonstration on this CT study. Surgical planning is facilitated by demonstrating these vascular-bone regional relationships.

For *ultrasonography* an Acuson 128 unit with 5 MHz linear array transducer was used.

Cadaveric model

Five cadaveric common carotid bifurcation–proximal internal and external carotid autopsy specimens were obtained from unselected elderly patients. The perivascular soft tissues were dissected away and the branches of the external carotid artery were ligated. However, when the external carotid artery appeared extensively diseased, ligation of the smaller branches became associated with leakage of the perfusate, thus ligation at the origin of the external carotid was needed.

The internal and external carotid artery branches were attached to the two upper limbs of a Y-adapter; the lower limb of the Y was attached to plastic tubing by silk suture material. The common carotid artery was also attached to additional plastic tubing which was then inserted into the track of a Harvard pump programmed to deliver 60 pulsations per minute. The two free ends of the tubing, i.e. that connected to the common carotid artery and that connected to the lower limbs of the Y-connector were immersed into a reservoir filled with water (collecting basin).

The cadaveric specimen was then placed in the center of a 'trough' made by splitting a plastic 1 liter bottle (Fig. 1). The plastic trough was then filled with water and the specimen and tubing submerged. Using air-filled syringes the immersed specimen and its connections were tested for leaks. If the system was found to be intact, all air was removed from the closed loop by aspiration.

When angiography was being assessed, a 5 F Hanaffee catheter was introduced into the system through a 5 ml 'vascular' sheath placed between the cadaveric bifurcation model and the Harvard pump.

After the angiography the collecting basin containing water was exchanged for a 0.2 % contrast medium filled container. The contrast medium was then pumped through the closed system and the CT examination was performed.

Patient examination

Seventeen patients with a history and examination consistent with carotid circulation ischemic disease had bilateral carotid angiography and serial dynamic ('fast scan') CT examination of the carotid bifurcations.

The patient lies supine on the CT table with the head restrained in a neutral position. A 300 ml bottle of 30 % contrast solution attached to a 22 G catheter was introduced into an antecubital vein. The initial flow was minimized to keep the vein patent. On a lateral CT scan the region to be examined was delimited: from the mid C5 vertebra to the mid C3 vertebra. The computer fast scan program was assigned to perform at the same parameters used for the cadaveric specimens. In the patient, usually 18 to 20 scans were obtained within two minutes. The patient had been instructed to maintain shallow breathing and to avoid swallowing during this period. Immediately prior to scanning, the patient received a bolus of 75 ml of contrast medium from the bottle using an air pressurization technique (2). The end of the 75 ml bolus signaled that scanning should be initiated during which administration of the contrast medi-

um was continued by either drip pressurization or by a CT injector programmed to deliver 1 ml/s. If the 18 to 20 initial scans satisfactorily covered the carotid bifurcation the examination was considered completed. In cases where additional sections were needed either more superiorly or inferiorly, the field was extended while providing an additional bolus of 50 ml of contrast medium. Thus, the total contrast volume used was usually 195 ml (and, occasionally, 245 ml).

The primary axial plane scans were followed by secondary multiplanar reconstructions. Various planes were explored to ascertain which would best display the morphologic course of the common carotid artery, internal and external carotid arteries. These axial CT data (in 3 cases) were also used to create the 3-D images.

All 17 patients had bilateral carotid angiography. The scale used to grade stenosis on CT, angiography, and pathologic evaluation is presented in Table 1.

3-D image contouring

The axial images were transferred via 9 track tape to the Cemax 1000 unit equipped with a 32-bit microprocessor, high resolution 1024 by 1280 line display system, and menu-driven software. The 3-D contour image forms a 'cast' of the intraluminal contrast of the distal common carotid artery and its proximal internal and external carotid branches. These contour images were displayed at various angular orientations for an optimal demonstration of the carotid bifurcation. In cases where calcified atheromatous plaques narrowed the vascular lumen the atheromatous calcifications were separately edited (identified by the operator) and displayed in a different color. Separate color densities were then selected, collated, and displayed.

The capability to rapidly rotate the accrued images best afforded visualization of the regional anatomy from any angle, but particularly enhanced 3-D perception. The most recently introduced software program is the 'transparency display program'. It makes the density of a particular anatomic structure more transparent to allow the display of its relationship to adjacent regional structure, i.e. a vessel to the 'overlying' spine, mandible, etc. (Figs 2, 3).

Results

Cadaveric model evaluation. Five cadaveric distal common carotid and proximal internal and external arteries were examined. A total of 13 of these 15 segments were examined since 2 external carotids required ligation (Table 2). Direct magnification film-screen and digital subtraction angiography were compared for detecting stenosis (Fig. 4 a, b). Both methods detected the same degree of stenosis at 7 of the 13 sites. However, of the ulcers found on digital subtraction angiography only one was seen on film-screen angiography. CT and gross pathologic inspection agreed in the degree of 8 stenotic areas within the 13 segments examined (Fig. 4 d, e). Both the CT and pathologic assessment showed 6 of the 8 stenotic segments to be more severely involved than on the angiographic evaluations. Moreover, one of the two ulcers seen on digital subtraction angiography and CT was not detected on gross pathologic evaluation (Table 2).

Table 1
Scale selected for grading stenosis

Grade	Stenosis	Per cent
0	None	0
1	Minimal	1–25
2	Mild	26–50
3	Moderate	51–75
4	Severe	76–99
5	Complete	100

Table 2
Cadaveric model. Angiographic and pathologic correlations of 5 carotid bifurcations (13 of 15 sites examined; 2 external carotid arteries were ligated)

Technique	Grade of stenosis						Ulceration
	0	1	2	3	4	5	
Directly magnified F-S angiography	6	5	2	0	0	0	1
DS angiography	6	5	2	0	0	0	2
CT with MPR and 3-D	5	2	4	2	0	0	2
Gross pathology	5	2	4	2	0	0	1

Table 3
Patient examination. Angiographic correlations in 34 carotid bifurcations

	Agreement between CT and F-S/DS angiography	Abnormalities demonstrated only on CT	Abnormalities demonstrated only on F-S DS angiography
Stenosis	22	9 + 2*	1 (kink)
Ulceration	7	–	2 (< 4 mm)
Vessel attenuation ('slim sign')	2	–	–
Precise site of complete occlusion	3	1	–
Detection of intra-luminal clot	–	2	–
Pseudoaneurysm	1	–	–

* Upgraded degrees of stenosis.

Patient evaluation

Thirty-four carotid bifurcations were evaluated (Table 3). One hundred and two sites (common carotid n = 34, internal carotid n = 34 and external carotid n =34) were evaluated by CT, F-S (8/17 patients) and/or DS (9/17 patients) angiography. The following processes were specifically searched for: degree of stenosis, ulceration, 'slim sign', pseudoaneurysm and intra-luminal thrombus. At 22

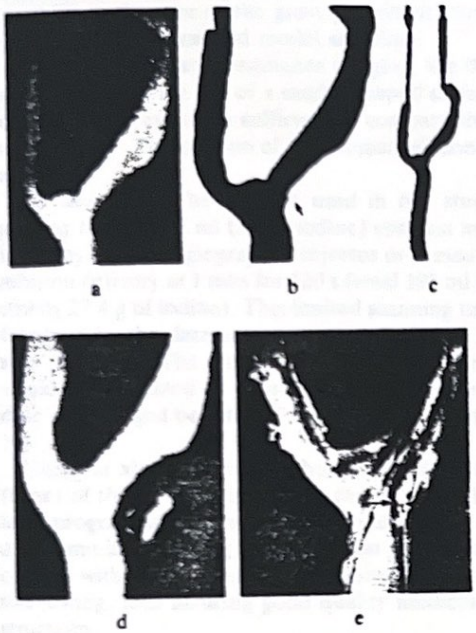

Fig. 4. Comparative imaging techniques of the carotid model. a) Film-screen angiography (Medichrome film photographed through orange filter). There is a smooth narrowing of the very proximal internal carotid artery. b) Digital subtraction angiography (15 % contrast medium; 70 mg I/ml). There is the same narrowing as in (a) but a discrete ulcer is well shown (arrow). c) Full length view of the model in (b). d) CT multiplanar reconstruction. There is again narrowing from the plaque, but the additional external contours of the vessel wall and its accompanying calcifications are now demonstrated. The carotid narrowing seems less on CT and there is minimal 'artefactual' staircase effect which is separable from the ulcerated mound (arrows). e) Gross pathology. Broad atheromatous plaque which has a cleft (arrows) several millimeters superior to the proximal extent of the plaque.

Fig. 5. Ultrasound imaging of the carotid model. This specimen was the best achieved and was normal at gross pathology.

sites there was corroborative agreement between the degree of stenosis on F-S/DS angiography and CT. At 9 sites stenosis was judged to be present by CT but not detected by F-S/DS angiography (6/19 were in distal common carotid arteries, 2/9 in external carotid arteries and 1/9 in internal carotid arteries). At 2 other sites (internal carotid, common carotid) more extensive stenosis was determined from CT than F-S/DS angiography. At only one other site was there more stenosis seen on DS angiography than on CT (due to kinking which was not possible to display by MPR enhanced CT). Of a total of 9 ulcerations, 7 were seen by both F-S/DS angiography and CT; however, 2 ulcers visualized on DS angiography were not detected on the CT component of the study (Table 3). Intra-luminal clot was readily and only demonstrable on CT. Otherwise, there was general accordance between F-S/DS angiography and CT in demonstrating precise detection of the site of complete occlusion, extensive narrowing with 'slim sign', and pseudoaneurysm of the internal carotid artery. In that case where angiography showed complete occlusion of the right common carotid artery, CT better defined the superior extent of the occlusion since it extended superiorly beyond the massive atheromatous calcification at the carotid bifurcation which did not demonstrate flow beyond it into the internal and external carotid arteries.

Discussion

The rapid availability of new or modified imaging options with variable invasive radiation techniques make clinical comparisons difficult. The model we propose and clinical studies comparing current techniques were undertaken. Perhaps, not surprisingly, some information confirmed our pre-investigation biases, while in other observations the results were unanticipated. This is the paradox of ulceration being better shown by CT in the model and better at angiography in the clinical situation. Nonetheless, this difference is within statistical variation.

Radiologic planning for the surgeon usually generates the following information; what vessels are involved, the length and magnitude of involvement, additional specific characterization as to ulceration and calcification, collateral vasculature, etc. The final morphologic arbiter pre-operatively has been catheter film-screen angiography. However, recent publications of CT findings (1, 4–10) question wheter the accepted reference standard is the appropriate standard of reference. Surgeons (3) have believed their visual observations to be the ultimate standard since the specimes they submit to the pathologist are delayed and only improvable by histologic examination. The presence of new imaging modalities would appear to raise the reliability of the radiologist in ascertaining morphologic information for the surgeon's use – the need for a reliable carotid model to assess the rapidly changing imaging techniques and the concomitant hardware and software support. A model must be tested to assure clinical concordance. This study therefore includes clinical material examined with the same imaging systems as used with the model.

The bottle containing the carotid model proved quite satisfactory for the angiographic and CT investigations. However, for ultrasound imaging the transducer proved too large for the bottle cutaway and the immersion depth of the model proved too shallow for convenient imaging, i.e. too close for the focal zone of the transducer to be effective. Two of the 5 models were imaged by us and one is included

(Fig. 5). A new container is being fabricated but was not available at the time of the gross pathologic corroboration of the bulk of the carotid model sampling.

Regarding magnetic resonance imaging, the 0.6 T Technicare unit with the aid of a saddle-shaped surface coil did not provide a resolution sufficient to compare the information with CT. This portion of the project will continue to be explored.

CT technique. The amount used in our studies was a priming bolus of 75 ml (30 % iodine) contrast medium followed by either 'angiographic' injector or pressurized rapid infusion delivery at 1 ml/s for 120 s (total 195 ml of 30 % or strictly 27.4 g of iodine). This limited scanning time was determined by the data storage available via the serial 'fast scan' program. The various doses cited in the literature would seem related to delivery technique. The minimum dose used ranged between 29.5 and 70 g of iodine (1, 4–7, 10).

Using the above outlined technique an adequate segment (6 cm) of the carotid bifurcation can be studied. The 'fast scan' program affords the acquisition of 18 to 20 axial scans over 2 minutes. During this time most patients are able to comply with the requests not to move and refrain from swallowing, thus assuring good quality multiplanar reconstructions.

Diagnostic value of the CT examination. Surgeons often indicate that angiography did not accurately portray what they found surgically, usually finding more stenosis than indicated by the catheter aided radiographic technique. Thus, not surprisingly, our cadaveric and patient studies corroborated with the results of others (1, 4–7, 10) showing that the cross-sectional display of the vascular lumen or axial CT scans is most accurate in providing degree of stenosis, extent of atheromatous calcification, and intraluminal clot.

Multiplanar and 3-D reconstructed images provide a morphologic display of vessels similar to the angiographic image. Moreover, these computer software produced images further improve the detection of ulcers, 'slim sign' and pseudoaneurysms.

Three-dimensional reconstructions have previously been used to improve the display of bony lesions. Due to the dense opacification of contrast medium in the lumen of a blood vessel, the 3-D software programs can also readily reconstruct a cast of this dense material as it did with bone.

Newly introduced 'transparency programs' (Cemax and Pixar) afford the display of two structures of similar density, i.e., the carotid arteries and the cervical spine. Their displays are from variable obliquities or cine rotation. Thus two overlapping similar radio densities become easily separable and perceptible from numerous viewing angles.

REFERENCES

1. Brant-Zawadzki M. and Jeffrey R. B. Jr: CT with image reformation for non-invasive screening of the carotid bifurcation. Early experience. Amer. J. Neuroradiol. 3 (1982), 395.
2. Burman S. and Rosenbaum A. E.: Rationale and techniques for intravenous enhandement in computed tomography. Radiol. Clin. N. Amer. 20 (1982), 15.
3. Edwards J. H., Kricheff I. I., Riles T. and Imparto A.: Angiographically undetected ulceration of the carotid bifurcation as a cause of embolic stroke. Radiology 131 (1979), 369.
4. Heinz E. R., Dubois P. and Drayer B.: Intravenous carotid imaging using the third dimension. Amer. J. Neuroradiol. 1 (1980), 363.
5. — Fuchs J., Osborne D. et coll.: Examination of the extracranial carotid bifurcation by thin-section dynamic CT. Direct visualization of internal atheroma in man. Part 2. Amer. J. Neuroradiol. 5 (1984), 361.
6. — Pizer S. M., Fuchs H. et coll.: Examination of the extracranial carotid bifurcation by thin-section CT. Direct visualization of internal atheroma in man. Part 1. Amer. J. Neuroradiol. 5 (1984), 355.
7. Iliya A. R., Hodge C. J., Leeson M. D. and Cacayorian E. C.: Carotid artery disease. Evaluation with CT scan. Annual meeting of the ASNR, Boston 1985.
8. Sartoris D. J.: 3-D display of CT data. New aid to preop surgical planning. Diagn. Imaging 5 (1986), 784.
9. Tress B. M., Davis S., Lavain J., Kane A. and Hopper J.: Incremental dynamic computed tomography. Practical method of imaging the carotid bifurcation. Amer. J. Neuroradiol. 7 (1986), 49.
10. Yamamoto M., Shinohara Y., Kamei T. and Yoshii F.: Diagnosis of internal carotid artery occlusion by dynamic computed tomography.